A bifunctional biased mu opioid agonist-neuropeptide FF receptor antagonist as analgesic with improved acute and chronic side effects

A bifunctional biased mu opioid agonist - neuropeptide FF receptor antagonist as analgesic with improved acute and chronic side effects

Armand Drieu la Rochelle[a#], Karel Guillemyn[b#], Maria Dumitrascuta[c#], Charlotte Martin[b], Valérie Utard[a], Raphaëlle Quillet[a], Séverine Schneider[d], François Daubeuf[d], Tom Willemse[b,e], Pieter Mampuys[e], Bert U.W. Maes[e], Nelly Frossard[d], Frédéric Bihel[d], Mariana Spetea[c**¶], Frédéric Simonin[a**¶] and Steven Ballet[b*¶]

Affiliations :

[a] Biotechnologie et Signalisation Cellulaire, UMR 7242 CNRS, Université de Strasbourg, Illkirch, France

[b] Research Group of Organic Chemistry, Departments of Chemistry and Bioengineering Sciences, Vrije Universiteit Brussel, Brussels, Belgium

[c] Opioid Research Group, Department of Pharmaceutical Chemistry, Institute of Pharmacy and Center for Molecular Biosciences Innsbruck (CMBI), University of Innsbruck, Innsbruck, Austria

[d] Laboratoire Innovation Thérapeutique, UMR 7200 CNRS, Université de Strasbourg, Illkirch, France

[e] Organic Synthesis, Department of Chemistry, University of Antwerp, Antwerp, Belgium

[#] Co-first authors

[¶] Co-senior authors

E-mail addresses: adrieularochelle@unistra.fr (A. Drieu la Rochelle), karelguillemyn@gmail.com (K. Guillemyn), maria.dumitrascuta@uibk.ac.at (M. Dumitrascuta), charlotte3martin@gmail.com (C. Martin), valerie.utard@unistra.fr (V. Utard), rquillet@unistra.fr (R. Quillet), schneider@unistra.fr (S. Schneider), francois.daubeuf@unistra.fr (F. Daubeuf), tomwille@vub.ac.be (T. Willemse); pieter.mampuys@uantwerpen.be (P. Mampuys), bert.maes@uantwerpen.be (B. Maes), nelly.frossard@unistra.fr (N. Frossard), mariana.spetea@uibk.ac.at (M. Spetea), fbihel@unistra.fr (F. Bihel), simonin@unistra.fr (F. Simonin), steven.ballet@vub.be (S. Ballet)

Correspondence:

* *Corresponding author - Medicinal chemistry. Research Group of Organic Chemistry, Departments of Chemistry and Bioengineering Sciences, Vrije Universiteit Brussel, Pleinlaan 2, 1050 Brussels, Belgium*

Tel: +32 2 6293292; Fax: +32 2 6293304; E-mail: steven.ballet@vub.be

** *Corresponding authors - Pharmacology*

Frédéric Simonin*: Biotechnologie et Signalisation Cellulaire, UMR 7242 CNRS/Université de Strasbourg. Ecole Supérieure de Biotechnologie de Strasbourg, 300, Boulevard Sébastien Brant - CS 10413 - 67412 Illkirch Cedex - France.*

Tel: +33 368 85 48 75; Fax: +33 368 85 46 83; E-mail: simonin@unistra.fr

Mariana Spetea: *Opioid Research Group, Department of Pharmaceutical Chemistry, Institute of Pharmacy and Center for Molecular Biosciences Innsbruck (CMBI), University of Innsbruck, Innsbruck, Austria*
Tel: +43 512 50758277; Fax: +43 512 50758299; E-mail: mariana.spetea@uibk.ac.at

Abbreviations:

AUC, area under the curve; BRET, Bioluminescence resonance energy transfer; cAMP, cyclic adenosine monophosphate; CFA, Complete Freund's Adjuvant; CHO, Chinese hamster ovary; DMF, dimethylfuran; Dmt, 2,6-dimethyltyrosine; DOPr, delta opioid receptor; HEK, human epithelial kidney; IBMX, 3-isobutyl-1-methylxanthine; KOPr, kappa opioid receptor; MOPr, mu opioid receptor; MPE, maximal possible effect; NOPr, nociceptin receptor; NPFF, neuropeptide FF; NPFFR, neuropeptide FF receptor; OIH, opioid-induced hyperalgesia; sc., subcutaneous; TFA, trifluoroacetic acid.

Abstract:

Opioid analgesics, such as morphine, oxycodone and fentanyl, are the cornerstones for treating moderate to severe pain. However, upon chronic administration, their efficiency is limited by prominent side effects such as analgesic tolerance and dependence liability. Neuropeptide FF (NPFF) and its receptors (NPFF1R and NPFF2R) are recognized as an important pronociceptive system involved in opioid-induced hyperalgesia and analgesic tolerance. Herein, we report the design of multitarget peptidomimetic compounds that show high affinity binding to the mu opioid receptor (MOPr) and NPFFRs. In vitro characterization of these compounds led to identification of KGFF03 and KGFF09 as G protein-biased MOPr agonists with full agonist or antagonist activity at NPFFRs, respectively. In agreement with their biased MOPr agonism, KGFF03/09 showed reduced respiratory depression in mice, as compared to the unbiased parent opioid agonist KGOP01. Chronic subcutaneous administration of KGOP01 and KGFF03 in mice rapidly induced hyperalgesia and analgesic tolerance, effects that were not observed upon chronic treatment with KGFF09. This favorable profile was further confirmed in a model of persistent inflammatory pain. In addition, we showed that KGFF09 induced less physical dependence compared to KGOP01 and KGFF03. Altogether, our data establish that combining, within a single molecule, the G protein-biased MOPr agonism and NPFFR antagonism, have beneficial effects on both acute and chronic side effects of conventional opioid analgesics. This strategy can lead to the development of novel and potent antinociceptive drugs with limited side effects upon acute and chronic administration.

Keywords:

Opioid receptors ; NPFF receptors ; RF-amide peptides ; opioid analgesia ; opioid-induced hyperalgesia ; analgesic tolerance ; physical dependence

1. Introduction

Opioids analgesics, such as morphine, oxycodone and fentanyl, continue to be cornerstone drugs for treating moderate to severe pain. Despite their undeniable benefit for treating severe acute pain, opioids still lack effectiveness for long-term therapy [9; 40; 55]. Indeed, repeated administration of opioids exacerbates adverse effects, such as pain hypersensitivity, which in turn impairs the analgesic efficacy and triggers the need for dose-escalation. In addition to pain hypersensitivity, risks of respiratory depression, addiction potential and constipation considerably affect the patient's quality of life [15]. In pursuit of safer analgesics, two main strategies recently emerged: G protein-biased mu opioid receptor (MOPr) agonists and multifunctional drugs with mixed opioid and non-opioid activities [21; 24; 37].

Research aiming at understanding the cellular and molecular mechanisms underlying the physiological analgesic response unveiled multiple pathways for MOPr activation and signaling. The signaling pathway coupled to heterotrimeric $G_{\alpha i/o}$ proteins inhibits downstream cAMP production, modulates activity of ion channels, and is ultimately responsible for pain relief. In addition to G protein, MOPr can activate parallel or distinct signaling pathways. β-Arrestin binding to the MOPr induces internalization, desensitization, as well as β-arrestin specific signaling, which is considered involved in opioid-induced respiratory depression, physical dependence, analgesic tolerance and constipation [7; 43; 44]. The potential of G protein-biased MOPr agonists, such as TRV130 and PZM21, has been extensively studied with promising preclinical and clinical results after acute administration [10; 25; 30; 31]. However, the consequences of chronic administration of such compounds have been poorly studied to date.

Another strategy to develop new analgesic drugs with an improved therapeutic profile has recently emerged, which consists in developing dual ligands acting both on the MOPr - to produce analgesia - as well as on other opioid or non-opioid receptors involved in pain

processing and/or opioid-induced side effects [11; 21; 32; 37; 52]. Among the non-opioid receptors, neuropeptide FF 1 and 2 receptors (NPFF1/2R) are recognized to contribute to the development of opioid-induced analgesic tolerance and other adverse effects [2; 4; 47]. NPFF has been shown to produce transient hyperalgesia, to reduce analgesic effect of morphine [56] and to potentiate opioid dependence [54], while pharmacological blockade of NPFF1/2R efficiently prevents the development of opioid-induced hyperalgesia (OIH), analgesic tolerance, and reduces morphine-induced withdrawal syndrome [14; 35; 48].

In light of these findings, the aim of our study was to generate peptidomimetic ligands combining potent MOPr agonist activity with NPFF1/2R antagonist activity. We describe here the identification and characterization of two interesting compounds, KGFF03 with agonist activity for the MOPr and NPFF1/2R, and KGFF09, a mixed MOPr agonist and NPFF1/2R antagonist. In vivo characterization of these compounds clearly shows that KGFF09 displayed reduced OIH, analgesic tolerance and withdrawal syndrome compared to KGFF03. Moreover, KGFF03 and KGFF09 displayed reduced respiratory depressive effects upon acute administration, a result probably related to their biased MOPr agonism. Altogether, these results establish KGFF09 as a potent analgesic drug with a reliable activity after chronic administration and a favorable safety profile, thus providing a promising therapeutic approach to tackle the present opioid epidemic [19].

2. Experimental procedures

2.1. Chemical Synthesis

Peptides KGFF01-KGFF07

Peptides KGFF01-KGFF07 were synthesized manually by standard Fmoc-SPPS on Rink amide AM resin. Standard couplings were performed with 3 equivalents (equiv.) of Fmoc-protected amino acid and 3 equiv. of coupling reagent (HCTU) in 0.4 NMM in DMF during 1.5 h. Fmoc-Aba-β-Ala-OH was coupled in only 1.5 equiv. excess of both Fmoc-dipeptide and coupling reagent for 3 h. Boc-Dmt-OH was coupled using 1.5 equiv. of amino acid and 1.5 equiv. of HOBt/DIC in DMF for 2 h, without addition of base to avoid coupling to the unprotected phenol group. For Fmoc-deprotection, the resin was treated with 20% 4-methylpiperidine in DMF for consecutively 5 and 15 min. Washing of the resin was performed after every coupling and after deprotection step with DMF (3x), iPrOH (3x) and CH_2Cl_2 (3x). Final cleavage and deprotection were done with the cleavage mixture (TFA/TES/H_2O 95:2.5:2.5) during 3 h. After filtration and concentration of TFA, the residue was added to cold ether to precipitate the peptide. The ether phase was decanted and the peptide was dissolved in acetonitrile/H_2O and lyophilized to obtain the crude peptides as a powder. The crude peptides were dissolved in H_2O and acetonitrile was added until complete dissolving was observed. This solution was injected on a Gilson preparative RP-HPLC. Fractions containing the product were combined and lyophilized. The final peptides were obtained with a purity >95% as white powders. The compounds were characterized by high-resolution electrospray mass spectroscopy.

Peptides KGFF08-KGFF11

The couplings of these four peptides were carried out using 3 equiv. of the amino acid with 3 equiv. of DIC/HOBt for 1.5 h in DMF. Coupling of both Fmoc-Aba-β-Ala-OH, Fmoc-Apa-OH and Fmoc-Bpa-OH were performed with only 1.5 equiv. of amino acid and coupling

reagent (DIC/HOBt) in DMF during 3 h. Boc-Dmt-OH was coupled with the same number of equivalents, but the reaction mixture was stirred only for 2 h.

Peptide KGFF12

The dipeptide Boc-Dmt-D-Arg(Pbf)-OH was first synthesized on 2-chlorotrityl chloride resin, using the same coupling and deprotection conditions as described above. Cleavage was performed with 1% TFA in CH_2Cl_2 to retain the side chain protective group. The solution was then evaporated and the dipeptide (1.1 equiv.) was dissolved in CH_2Cl_2. Two equiv. DIPEA and 1.5 equiv. DIC/HOBt were added and the mixture was stirred for 30 min at 0°C. The free 4-amino-Aba-NH was added and stirred for another 30 min in an ice bath. The reaction was then left on stirring during 16 h at room temperature. After this coupling, the protective groups were removed with the same cleavage cocktail as described for the preparation of peptides KGFF01-KGFF07, and purification was performed analogously.

Peptide KGFF13

This synthesis was performed on FMPB-AM resin (4-(4-formyl-3-methoxyphenoxy)butyrylaminomethyl resin). Methylamine hydrochloride (10 equiv.) was coupled to the aldehyde resin by a reductive amination with sodium cyanoborohydride (10 equiv.) in MeOH/DMF for 2.5 h at 80°C. Complete coupling was determined by the DNPH-color test. Further standard SPPS coupling, cleavage and purification were performed as described for peptides KGFF01-KGFF07 (*vide infra*).

Peptides KGFF14-KGFF16

These 3 peptides were synthesized on MBHA-resin. The couplings (Boc-Dmt-OH, Boc-D-Arg(Tos)-OH, Boc-Phe-OH) were performed with 3 equiv. of amino acid and 3 equiv. of coupling reagent (HCTU) in 0.4 NMM in DMF for 1.5 h. Both the arginine mimetics and Boc-Dmt-OH were coupled with DIC/HOBt in DMF with respectively 1.5 (Arg mimetics) and 2 equiv. of amino acid and coupling reagent. Fmoc-Aba-β-Ala-OH was coupled with 1.5

equiv. of HCTU in 0.4 NMM in DMF for 3 h. This Fmoc-group was removed as described above. The Boc-deprotection was performed with 50% TFA in CH_2Cl_2 for 5 and 15 min and washed as previously described. The neutralization step after every Boc-deprotection was realized with a solution of 20% triethylamine in CH_2Cl_2 during 10 min (2 times). Final cleavage was done with liquid HF (10 mL/g resin) and anisole (0.5 mL per 50 mg resin) as scavenger for 1 h at 0°C. After HF distillation, cold ether was added to precipitate the peptides. The peptides were filtered and dissolved in acetic acid/H_2O, and lyophilized. The white powders could be purified by preparative RP-HPLC. Only in case of the paramethoxybenzyl-protected benzoimidazole-containing peptide (KGFF14), an extra step had to be performed to fully cleave the protective group: the peptide was treated with 10% triflic acid (0.5 mL) in TFA (4.5 mL) for 4 h, the solvent was evaporated and the product was purified by preparative RP-HPLC.

Peptide characterization and synthesis of the arginine mimetics and ornithine mimetics are described in *Materials and Methods Supplemental Digital Content 1.*

2.2. Receptor cDNA constructs, cell expression and membrane preparations

Human embrionic kidney 293 (HEK293) cells expressing Glo-sensor 20F were a gift from M. Hanson (GIGA, Liège, Belgium). Human MOPr, DOPr, KOPr, NOPr, NPFF1R, NPFF2R and GPR54 cDNAs were subcloned into the pCDNA3.1 expression vector (Invitrogen, Cergy Pontoise, France) and transfected into Chinese Hamster ovary (CHO) cells or HEK293-Glo-20F cells before selection for stable expression, as reported [13]. CHO cells expressing human GPR10 and GPR103 were a gift from M. Parmentier (IRIBHM, Brussels, Belgium). All cell membranes were prepared as described [13], and stored at –80°C as aliquots (1 mg protein/mL) until use.

2.3. Radioligand binding assays

Binding assay conditions were essentially performed as described [13]. Briefly, membranes from CHO cells stably expressing human GPR10, GPR54, GPR103, NPFF1R or NPFF2R were incubated with 0.6 nM [^{3}H]-PrRP-20, 0.05 nM [^{125}I]-Kp-10, 0.03 nM [^{125}I]-43RFa, or 0.015 nM [^{125}I]-1-DMe-NPFF (for NPFF1R and NPFF2R), respectively. Membranes from HEK293 cells stably expressing human MOPr, DOPr and KOPr were incubated with 1 nM [^{3}H]-diprenorphine. Membranes from HEK293 cells transiently expressing human NOPr were incubated with 0.2 nM [^{3}H]-nociceptin. Competition binding experiments were performed at 25°C, under equilibrium conditions (60 min, 0.25 mL final volume), in the presence of increasing concentrations of unlabeled peptides or test compounds. Membrane-bound radioactivity was separated from free radioligand by rapid filtration through a 96-well GF/B unifilter apparatus (Perkin Elmer Life and Analytical Sciences, Courtaboeuf, France) and quantified using a TopCount scintillation counter (Perkin Elmer).

2.4. [^{35}S]-GTPγS binding assay

Stimulation by endogenous RF-amide peptides or test compounds for [^{35}S]-GTPγS binding to membranes from CHO cells expressing human NPFF1R or NPFF2R, were examined as reported [48].

2.5. Glo-sensor cAMP assay

cAMP accumulation assay was essentially done as described [45] with the following modifications: HEK293 cells stably expressing cAMP Glosensor-20F were used, with or without additional stable expression of each individual opioid receptor or NPFF1R. The cAMP responses were measured in presence of D-luciferin (1 mM). All peptides and test compounds were incubated in the presence of IBMX for 15 min before inducing cAMP

production by forskolin. IBMX and forskolin concentrations were optimized for each receptor cell line: NPFF1R responses were recorded in presence of 0.1 mM IBMX and 0.4 µM forskolin; MOPr with 0.5 mM IBMX and 0.125 µM forskolin; DOPr responses with 0.1 mM IBMX and 0.125 µM forskolin; KOPr and NOPr with 0.5 mM IBMX and 1.5 µM forskolin.

2.6. Calcium mobilization assay

CHO cells expressing human NPFF2R were loaded with 2.5 µM Fluo-4 AM in the presence of 2.5 mM probenecid, as described previously [13]. Agonist-evoked increases in intracellular calcium were recorded over time (5 sec intervals over 220 sec) at 37°C through fluorescence emission at 520 nm (excitation at 485 nm). Peak response amplitudes were normalized to basal and maximal (cells permeabilized with 20 µM digitonin) fluorescence levels.

2.7. β-Arrestin-2 recruitment assay

The β-arrestin-2 recruitment assay was performed as described [34; 45] with minor modifications. Briefly, two days prior the experiment, HEK293 cells stably expressing eYFP-tagged β-arrestin-2 were transfected with the plasmid encoding Rluc8-MOP receptor. β-Arrestin-2 recruitment was measured at 37°C in presence of 5 µM Coelenterazine H, 5 min after agonist addition. A "BRET ratio" corresponding to the signal in the "acceptor channel" (band-pass filter 510-560 nm) divided by the signal in the "donor channel" (band-pass filter 435-485 nm) was calculated. Drug-induced BRET was determined (BRET1 ratio of drug-activated cells minus BRET1 ratio of buffer-treated cells) and normalized to the maximum of DAMGO-induced BRET, defined as 100%.

2.8. In vivo experiments

All experiments were carried out in accordance with the European guidelines for the care of laboratory animals (European Communities Council Directive 2010/63/EU) and were

approved by the local ethical committee and authorized by the French Ministry for Research and the Committee of Animal Care of the Austrian Federal Ministry of Science and Research. All efforts were made to minimize animal discomfort and to reduce the number of animals used.

2.9. Animals

Animal experiments were performed on adult male C57BL/6N male mice (25-30 g weight; Janvier labs, France) and CD1 mice (30-35 g body weight; Center of Biomodels and Experimental Medicine (CBEM), Innsbruck, Austria). Animals were housed in groups of three to five per cage and kept under a 12 h/12 h light/dark cycle at 21 ± 1°C with *ad libitum* access to food and water. Experiments were performed during the light-on phase of the cycle. Mice were habituated to the testing room and equipment before starting behavioral experiments. Control and treated group assignment as well as pain response measurements were performed in a blinded manner. Every animal was used only once.

2.10. Drug administration

All drugs were dissolved in physiological saline (0.9%) and administered subcutaneously (sc.) at 10 mL/kg (volume/body weight).

2.11. Assessment of thermal nociception

The nociceptive sensitivity to thermal stimulation was determined in mice using the radiant heat tail-flick and 47.5°C warm-water tail immersion tests as previously described [12; 36; 49]. The tail-flick test was performed in CD1 mice using the UB 37360 Ugo Basile analgesiometer (Ugo Basile s.r.l., Varese, Italy), where the reaction time required by the mouse to remove its tail after application of the radiant heat was measured and defined as the

tail-flick latency (in sec). A cut-off time of 10 sec was used in order to minimize tissue damage. In the tail immersion test, C57BN/6N mice were restrained in a grid pocket and their tail was immersed in a thermostated water bath. The latency (in sec) for tail withdrawal from hot water (47.5 ± 0.5°C) was taken as a measure of the nociceptive response. In the absence of any nociceptive reaction, a cut-off value of 25 sec was set to avoid tissue damage.

Experiments for acute drug effect were designed according to a protocol enabling the evaluation of the time course of the antinociception response of test compounds. Nociceptive latencies were determined before (baseline) and after drug or saline (control) sc. administration (i.e. 15 min, 30 min, and every hour up to 8 h, and 24 h). Dose-response curves were constructed for test compounds. Antinociceptive response was calculated as percent of Maximum Possible Effect (%MPE) according to the formula = [(test latency – baseline latency)/(cut-off time – baseline L)] x 100. The dose necessary to produce a 50% MPE (ED_{50}) and 95% confidence limits (95% CL) were calculated.

Experiments for chronic drug effects were designed according to a protocol enabling the evaluation of time course of opioid-induced hyperalgesia and development of analgesic tolerance using the tail immersion test. C57BL/6N mice were sc. treated daily with 1.8 µmol/kg/d KGOP01, 1.2 µmol/kg/d KGFF03, 7.4 µmol/kg/d KGFF09 or saline (controls) for 8 days. For analgesic tolerance evaluation, nociceptive latencies were measured on day 1 and 8 according to the acute effect protocol. For the assessment of hyperalgesia, basal nociceptive latencies were measured every day, 30 min before drug or saline injection. Responses are expressed as latency times (in sec) of tail withdrawal from the hot water.

2.12. CFA-induced inflammatory pain model

Tail inflammation in C57BL/6N mice was induced by injecting subcutaneously 20 µl of a Complete Freund's Adjuvant (CFA) solution or saline (control mice), 3 cm from the tip of the tail [41]. Twenty-four hours after CFA injection (day 1), inflammation was confirmed by

measuring thermal and mechanical hyperalgesia. Mice were then treated sc. daily for 7 days (from day 1 to day 7) with the test compounds or saline (control). Nociceptive threshold to heat stimulation was measured by tail immersion test (47.5 ± 0.5°C) and tail pressure test [12] each hour for 5 h after the first drug administration in order to determine the peak of the anti-hyperalgesic response. During the following days, basal nociceptive thresholds were evaluated before and 2 h after drug injection. Antinociceptive response was calculated as %MPE according to the formula = [(test latency – CFA/saline mice latency)/(cut-off time – CFA/saline mice latency)] x 100. In order to limit behavioral sensitization, thermal nociception was evaluated on days 1 - 2 - 4 - 6, and mechanical nociception was evaluated on days 1 - 3 - 5 - 7.

2.13. Naltrexone-precipitated withdrawal syndrome

Opioid physical dependence was induced in C57BL/6N mice by sc. administration of test compounds twice daily, 1.8 µmol/kg KGOP01, 1.2 µmol/kg KGFF03, 7.4 µmol/kg KGFF09 or saline (control) over a 7-days period. On day 7, two hours after the last drug injection, the withdrawal syndrome was precipitated by administration of naltrexone (5 mg/kg, sc.) and evaluated over 30 min. Jumping, paw tremors and wet dog shakes were recorded as number of events occurring during the total test time. Diarrhea was checked for 30 min with one point given for any signs of it during each 5 min period (maximum score: 6). Body weight was measured immediately before and after each 30 min test session, and percentage of body weight lost was calculated. For each mouse, a global opiate withdrawal score was also calculated by summing the values obtained for each sign. For this purpose, one point was assigned to every 3 jumps and 5 paw tremors, respectively, whereas all other signs were given the absolute values recorded during the test [39].

2.14. Respiratory depression measurement using whole body plethysmography

Ventilatory parameters were recorded in conscious C57BL/6N mice by whole body barometric plethysmography (Emka Technologies, Paris, France). Mice were acclimatized with the plethysmograph chamber for 30 min until a stable baseline was obtained. Then, the animal was gently removed from the chamber for sc. injection of the tested drug at T_0 and replaced in the chamber for the remaining measurements. Respiratory frequency (f) was recorded for 100 min and used as the index of respiratory depression [31].

2.15. Colonic bead exclusion test for assessment of gastrointestinal motility

Colonic bead expulsion test was used to assess the effect of test compounds on gastrointestinal motility in CD1 mice as described previously [26]. Thirty minutes after sc. administration of test compounds or saline (control), a single 2 mm glass bead was inserted 1.5 cm into the distal colon using a silicon pusher. After bead insertion, mice were placed in individual plastic boxes, and the time required for expulsion of the glass bead was determined for each animal. The time required to expel the bead was measured up to 120 min.

2.16. Rotarod test for assessment of motor coordination

Possible motor dysfunction or sedative effects of test compounds were assessed in CD1 mice using the rotarod test as described previously [51]. The accelerating rotarod treadmill (Acceler Rota-Rod 7650, Ugo Basile s.r.l., Varese, Italy) for mice (diameter 3.5 cm) was used. Animals were habituated to the equipment in two training sessions (30 min apart) one day before testing. On the experimental day, mice were placed on the rotarod, and the treadmill was accelerated from 4 to 40 rpm over a period of 5 min. The time spent on the rod was recorded for each mouse before and after test compound or saline (control) sc. administration (i.e. 30 min and every hour up to 8 h, and 24 h). Decreased latencies to fall from the rotarod indicate impaired motor performance. A 300 s cut-off time was used.

2.17. Statistics

For in vitro binding and functional experiments, two to four independent experiments were performed in duplicates and data were analyzed using Prism (GraphPad Software, San Diego, CA, USA). In vivo data are expressed as mean values ± SEM for 6 to 12 mice per group. Antinociception was quantified as the area under the curve (AUC) calculated by the trapezoidal method [8]. Data were analyzed using one-way or two-way analysis of variance (ANOVA). Post-hoc analyses were performed with Bonferroni tests. The level of significance was set at $p < 0.05$. All statistical analyses were carried out using the StatView or GraphPad Prism softwares.

3. Results

3.1. Design strategy and biological screening of MOPr/NPFFR peptidomimetic ligands

In this study, we designed a series of bifunctional ligands that were based on a combination of the recently described MOPr peptidomimetic KGOP01 [20], found to display potent analgesic activity following systemic administration, and standard but also more evolved NPFF pharmacophores (Fig. 1 *A* and *B*). The sequences of synthetized peptidomimetics are shown in Table 1. As a standard NPFF pharmacophore, the *C*-terminal RF-NH_2 dipeptide segment of NPFF served as a minimal recognition motif (structure 2, Fig. 1*A*). Many of the reported NPFF analogues contain the *C*-terminal Arg-Phe-amide, derived with an apolar moiety linked at its *N*-terminus [16; 18; 23; 33; 48]. Combination of both pharmacophores (Table 1) afforded KGFF01 and KGFF03 that showed nanomolar affinity for MOPr and NPFF1/2R (Fig. 1*C* and Table Supplemental Digital Content 2, which summarize affinity constant (K_i) values of KGFF compounds for MOPr, NPFF1R, and NPFF2R). The amino-benzazepinone (Aba) scaffold could act as the apolar group that is often present in previously reported NPFF ligands. The insertion of a Gly (KGFF01) or a β-Ala (KGFF03) in position 4, i.e. between the RF-NH_2 dipeptide and the benzazepinone ring, provided good affinity for NPFF1/2R with preserved MOPr affinity, while eliminating a potential steric hindrance imposed by the NPFF pharmacophore onto the opioid part. The corresponding *C*-terminal carboxylic acid (KGFF02) confirmed the importance of the *C*-terminal amide in this type of hybrid with a strong decrease of affinity for both NPFF1/2R. Likewise, the substitution of the Arg residue by Orn (KGFF04, KGFF05) was not well tolerated, resulting in reduced binding affinities to both NPFF1/2R subtypes (Fig. 1*C* and Table Supplemental Digital Content 2, which summarize affinity constant (K_i) values of KGFF compounds for MOPr, NPFF1R, and NPFF2R).

Further truncation of KGFF01 gave way to tripeptides KGFF06 and KGFF07 with complete overlap of the opioid and NPFF pharmacophores, as the 2,6-dimethyl tyrosine

(Dmt) side chain could efficiently serve as the apolar group. In this case, the opioid segment is cut down to three amino acids instead of four, with well-conserved MOPr binding affinity for KGFF07. In addition to the detrimental consequence on MOPr affinity, the stereochemistry of Arg (L-Arg for KGFF06 and D-Arg for KGFF07) seems to drive a selectivity switch between NPFF1R and NPFF2R (Fig. 1*C* and Table Supplemental Digital Content 2, which summarize affinity constant (K_i) values of KGFF compounds for MOPr, NPFF1R, and NPFF2R).

Following initial in vitro biological evaluation of the described hybrid peptidomimetics, the two peptide analogues, KGFF03 and KGFF07, with the most promising binding data on MOPr and NPFFR were used to design a second set of bifunctional peptides (Table 1). Within this second set, the Arg residues were replaced by both reported Orn-derivatives (Fig. 1*B*, **3**, **Apa** [2-**a**mino-5-(piperidin-1-yl)**p**entanoic **a**cid] and **4**, **Bpa** [2-amino-5-(4-**b**enzylpiperidin-1-yl)**p**entanoic **a**cid]) [46], as well as novel Arg mimetics (**5** to **7**, Fig. 1*B*). Structural modifications on KGFF07 were first explored. Substitution of L- or D-Arg[2] by **3** and **4** using standard Fmoc-SPPS gave rise to tripeptide analogues KGFF10 and KGFF11, with a consequential dramatic loss of affinity for MOPr and NPFFR. In an attempt to lower the molecular flexibility of this tripeptide, the *C*-terminal Phe was constrained through incorporation of the Aba core (KGFF12), resulting in a significant drop in binding affinity for NPFF1R and to a lesser extent for NPFF2R. In order to verify if the decrease in affinity was due to the incorporation of the methylene bridge providing the cycle or from the conversion of a primary to a secondary amide, the 'open ring' analogue KGFF13 was also synthetized. This compound displayed a partially restored affinity for the NPFF1R and NPFF2R (Fig. 1*C* and Table Supplemental Digital Content 2, which summarize affinity constant (K_i) values of KGFF compounds for MOPr, NPFF1R, and NPFF2R).

We have recently shown that the guanidine moiety of Arg can be advantageously replaced by tertiary amines in the sequence RF-NH_2, leading to new peptidomimetic ligands of NPFFRs [5]. Based on the promising biological data on KGFF01 and KGFF03, and in light of our previous work, the Arg^5 residue was replaced by piperidine- and benzylpiperidine-bearing residues **3** and **4**, respectively (Fig. 1*B*), to give the hybrid products KGFF08 and KGFF09 (Table 1). The Arg mimetics (**5** to **7**) were incorporated at the same position in this sequence leading to KGFF14, KGFF15 and KGFF16 (Table 1). Substitution of Arg^5 in KGFF03 with these Arg mimetics led in general to good binding affinity for both MOPr and NPFF1/2Rs (MOPr: K_i < 10 nM; NPFF1R: K_i < 150 nM; NPFF2R: K_i < 15 nM) with a globally better affinity for the NPFF2R over NPFF1R subtype, especially after incorporation of Apa, Bpa and Lys(Box) residues. Based on these data, hybrid peptidomimetics KGFF01/-03/-07/-08/-09/-14/-15/-16 were selected for further characterization of their activity at MOPr and NPFF1/2R in functional assays.

3.2. Identification of an MOPr/NPFFR agonist (KGFF03) and a mixed MOPr agonist / NPFFR antagonist (KGFF09)

We first evaluated the capacity of the selected compounds to inhibit forskolin-induced cAMP production from MOPr overexpressing HEK293 cells. All ligands displayed full agonist activity at the MOPr (EC_{50} values ranging from 1.5 to 18.2 nM, as compared to DAMGO, EC_{50} = 80 nM, Fig. 2*A* and Table Supplemental Digital Content 3, which summarize agonist activity constants (EC_{50} and E_{max}) values of KGFF compounds for MOPr, NPFF1R, and NPFF2R). We then evaluated the functional activity of the KGFF compounds on both NPFF1R and NPFF2R in the [^{35}S]-GTPγS binding assay (Fig. 2 *B* and *C*, and Table Supplemental Digital Content 3, which summarize agonist activity constants (EC_{50} and E_{max}) values of KGFF compounds for MOPr, NPFF1R, and NPFF2R). KGFF03 was the most

potent agonist for both NPFF1/2R (NPFF1R: EC_{50} = 84.8 nM; NPFF2R: EC_{50} = 11 nM), whereas KGFF09 was the only ligand to show no or weak agonist activity at both NPFF1R and NPFF2R. We further confirmed the absence of agonist activity of KGFF09 on NPFFRs by using integrated cellular assays (Figure Supplemental Digital Content 4 *A* and *C*, which shows in vitro characterization of KGFF03 and KGFF09 on NPFFRs). Finally, we showed that KGFF09 displayed potent antagonist activity at NPFF1/2Rs (Fig. 2 *E* and *F*, Figure Supplemental Digital Content 4 *B* and *D*, which shows in vitro characterization of KGFF03 and KGFF09 on NPFFRs) with pA_2 values of 7.25 ± 0.30 and 7.77 ± 0.21, respectively, calculated from [^{35}S]-GTPγS binding experiments.

Overall, these data allowed us to identify one molecule, KGFF03, that displays potent MOPr and NPFFR agonist activities, and a second ligand, KGFF09, that shows mixed MOPr agonist and NPFF1/2R antagonist activities. These two ligands underwent further in vitro and in vivo characterization, and their profiles were compared to the parent opioid ligand KGOP01.

3.3. KGFF03 and KGFF09 are G protein-biased MOPr agonists

While opioid-induced analgesia is attributed to MOPr signaling through the G protein G_i, β-arrestin-2 recruitment upon MOPr activation is proposed to be responsible for many acute side effects including respiratory depression and constipation [10; 31; 43]. To examine MOPr biased agonism of KGOP01, KGFF03 and KGFF09 towards activation of G protein- over β-arrestin-2-mediated signaling, we compared their functional activity, i.e. potency and efficacy, across two cell-based assays that measure G protein coupling (the cAMP accumulation assay) and β-arrestin-2 translocation (the BRET1 β-arrestin-2 recruitment assay) at the human MOPr (Fig. 2 *A* and *D*, Table Supplemental Digital Content 3, which summarize agonist activity constants (EC_{50} and E_{max}) values of KGFF compounds for MOPr, NPFF1R, and NPFF2R, and

Figure Supplemental Digital Content 5, which shows the robustness of β-arrestin-2 recruitment to MOPr induced by DAMGO). Both KGFF03 and KGFF09 elicited partial agonism for β-arrestin-2 recruitment, while being highly potent and fully efficacious in promoting MOPr-induced G protein activation. In contrast, KGOP01 robustly stimulated interaction between the MOPr with G protein and β-arrestin-2 with a full response and potency, as compared to DAMGO. These data indicate that the two newly designed MOPr/NPFFR hybrid ligands, KGFF03 and KGFF09, activate MOPr in a manner that is preferentially biased toward G protein signaling.

3.4. Selectivity of KGFF03 and KGFF09 at opioid and RF-amide receptors

We further investigated the binding affinity and functional activity of KGFF03, KGFF09 and KGOP01 at other opioid receptor types (Table 2 and Figure Supplemental Digital Content 6, which shows in vitro characterization of KGOP01, KGFF03 and KGFF09 on opioid receptors). KGFF03 showed good affinity at the DOPr, and lower affinity for KOPr and NOPr. It displayed potent agonist activity at DOPr (EC_{50} = 0.34 nM) and lower agonist activity at KOPr (EC_{50} = 95 nM), as well as very weak antagonist activity at NOPr (pA_2 = 5.3 ± 0.34). KGFF09 showed lower affinity at the DOPr and relatively higher affinity for the KOPr, in comparison with KGOP01 and KGFF03. Its affinity for the NOPr was similar to KGFF03. Alike KGOP01 and KGFF03, KGFF09 displayed potent agonist activity at DOPr (EC_{50} = 0.78 nM). Moreover, KGFF09 displayed potent antagonist activity at the KOPr (pA_2 = 8.16 ± 0.13), but low antagonist activity at the NOPr (pA_2 = 5.94 ± 0.12).

Because NPFFRs belong to the family of RF-amide receptors, which include GPR10, GPR54 and GPR103 [13], we also evaluated selectivity of our compounds for these receptors. KGOP01, KGFF03 or KGFF09 displayed no or low binding affinity for GPR10, GPR54 and

GPR103 (Table Supplemental Digital Content 7, which summarize affinity constant (K_i) values of KGFF compounds for GPR10, GPR54 and GPR103).

3.5. Acute subcutaneous administration of KGFF03 and KGFF09 produces dose-dependent, long-lasting antinociception in mice

We evaluated the acute antinociceptive activity of the new MOPr/NPFFR hybrid structures, KGFF03 and KGFF09, in two mouse models of thermal acute nociception after sc. administration and compared them to the parent opioid, KGOP01. All three peptides produced time- and dose-dependent increase in tail withdrawal latencies in the tail immersion test (Fig. 3*A*) and the radiant heat tail-flick test (Fig. 3*B*), with KGFF03 and KGFF09 showing a prolonged antinociceptive response (Fig. 3*B*). The established profile in this study for KGOP01 following sc. administration is similar to that recently reported in the tail-flick test after intravenous administration in mice [20]. The ED_{50} values of the tested peptidomimetics at the peak of action are shown in Table 3. When compared to KGOP01, KGFF03 was equipotent whereas KGFF09 was 4.5-fold less potent in inducing antinociception, in agreement with its slighly lower affinity for the MOPr (Fig. 1*C*). Morover, the potency of the three compounds was several fold higher than that of the gold-standard opioid analgesic morphine (Table 3).

3.6. Chronic subcutaneous administration of KGFF09 does not induce hyperalgesia nor analgesic tolerance in naïve mice

To evaluate if the blockade of the NPFF system prevents the development of hyperalgesia and analgesic tolerance, mice were chronically administered equianalgesic doses of either KGOP01, KGFF03 or KGFF09, as shown in the time course of analgesia on day 1 of the chronic administration scheme (Fig. 4*A*). When sc. administered at a dose of 1.8 µmol/kg/d,

KGOP01 produced a significant and progressive decrease of the basal thermal nociceptive threshold, compared with control saline-treated animals (Fig. 4*B*). This effect was significant from the fifth day of the daily administration and persisted until the end of the experiment. As shown in Figure 4 (*A* and *B)*, chronic administration of KGFF03 (1.2 µmol/kg/d, sc.) resulted in a similar development of thermal hypersensitivity, a trend that was absent in mice treated with KGFF09 (7.4 µmol/kg/d, sc.). In the same study, we measured the antinociceptive effect of each compound on days 1 and 8 (Fig. 4 *A* and *C*). On day 1, KGOP01, KGFF03 and KGFF09 induced full antinociception (maximal response reaching almost the 25 s cut-off limit). On day 8, mice treated with either KGOP01 or KGFF03 showed a reduction of maximal response and a decrease in the antinociception efficacy (defined by the AUC) by more than 75% compared to day 1 (Fig. 4*C*), indicating that tolerance developed upon chronic administration. Conversely, the maximal analgesia induced by KGFF09 was maintained from day 1 to day 8, with a decrease of analgesic efficacy (AUC) on day 8 by less than 25% as compared to day 1. These data clearly indicate that blocking NPFF1/2Rs in addition to the MOPr activation leads to potent analgesia without development of tolerance upon chronic administration.

3.7. KGFF09 displays reduced withdrawal syndrome and respiratory depression

We further studied the development of naloxone-precipitated withdrawal syndrome after chronic sc. administration to mice of KGOP01, KGFF03 and KGFF09. Mice were treated twice a day over a 7 days period with the same doses used in previous experiments. Administration of naltrexone (1 mg/kg, sc.), 2 h after the last injection of KGOP01, induced high scores on several somatic and vegetative signs in the drug-dependent mice, as compared to the control saline-treated animals (Figure Supplemental Digital Content 8, which shows effect of KGOP01, KGFF03 and KGFF09 on naltrexone-precipitated withdrawal signs after

chronic exposure in mice). A similar withdrawal profile was observed for KGFF03, while all signs of withdrawal were reduced following chronic administration of KGFF09 (Figure Supplemental Digital Content 8, which shows effect of KGOP01, KGFF03 and KGFF09 on naltrexone-precipitated withdrawal signs after chronic exposure in mice). Analysis of the global opiate withdrawal score revealed that withdrawal was significantly reduced (to ca. 50%) after KGFF09 chronic administration, in comparison to KGFF01 and KGFF03 (Fig. 4*D*). This result is in agreement with our previous report, showing reduced morphine withdrawal upon administration of the NPFF1/2R antagonist RF9 [14; 48].

We next studied respiratory depression and constipation, two main side effects that occur upon acute opiate administration. As shown by the measurement of respiratory frequency (Fig. 4*E*), KGOP01 produced significant respiratory depression compared to saline-treated animals, while KGFF03 and KGFF09 did not. This result is in agreement with previous reports suggesting that respiratory depression is strongly associated with the β-arrestin-2 recruitment by the MOPr [10; 31]. Conversely, neither KGFF03 nor KGFF09 were able to alleviate opioid-related constipation, as measured by an extended bead expulsion time in mice (Figure Supplemental Digital Content 9*A*, which shows effect of KGOP01, KGFF03 and KGFF09 on gastrointestinal motility). Finally, other behavioral observations revealed that, unlike KGOP01 and KGFF03, at the first administration of the highest dose, KGFF09 (7.4 µmol/kg, s.c.) induced a transitory lethargic state with an impaired motor coordination in mice (Figure Supplemental Digital Content 9*B*, which shows effect of KGOP01, KGFF03 and KGFF09 on motor coordination) that was not observed upon repeated administration.

3.8. KGFF09 chronic administration efficiently reverses CFA-induced hyperalgesia

Additionally, we characterized the analgesic profile of our compounds in a mouse model of persistent inflammatory pain induced by sc. injection of CFA in the tail of mice on day 1.

Animals were then daily sc. administered equianalgesic doses of KGOP01 (1.8 µmol/kg/d), KGFF03 (1.2 µmol/kg/d) or KGFF09 (7.4 µmol/kg/d) from day 2 to day 8, and their activity upon thermal or mechanical nociceptive stimulation was measured on days 2, 3, 5 and 7 for the thermal stimulus, and on days 2, 4, 6, 8 for the mechanical stimulus. Measurements were performed 2 h after each daily drug injection. Under these conditions, we observed that nociceptive threshold of animals injected with KGOP1, KGFF03 and KGFF09 not only returns to basal nociceptive values but raises above the basal threshold, indicating that these compounds displayed, not only anti-hyperalgesia, but also antinociceptive activity (Figure Supplemental Digital Content 10, which shows acute antinociceptive time course of KGOP01, KGFF03 and KGFF09 in CFA-induced pain model). For this reason, results from Figure 5 (*A* and *B*) were considered as antinociception rather than anti-hyperalgesia. As shown in Figure 5 (*A* and *B*), both thermal and mechanical antinociception induced by KGOP01 and KGFF03 rapidly decreased after repeated administrations, with decreased analgesia compared to day 1 (> 75%), clearly showing that these two compounds led to the development of analgesic tolerance. In contrast, KGFF09 preserved the potent analgesic effect, with significantly less tolerance after 7 days of chronic administration (Fig. 5 *A* and *B*). Because KGFF09 alleviate opioid-induced hyperalgesia upon chronic administration (Fig. 4 *A* and *B*), we tested if this was true for CFA-induced hyperalgesia. To this purpose, basal nociceptive thresholds of the animals were measured daily before injection of the compounds (Fig. 5 *C* and *D*). The thermal hypersensitivity induced by CFA was reduced after a single administration of KGFF09, and totally reversed after the third injection (Fig. 5*C*), which was not the case with KGOP01 and KGFF03. Likewise, the basal mechanical nociceptive threshold of mice gradually returned to normal after repeated administration of KGFF09 (Fig. 5*D*), but not after KGOP01 and KGFF03. Overall, our data demonstrate that in a model of persistent inflammatory pain,

blockade of NPFF1/2Rs preserves opioid analgesia upon repeated administration and allows efficient reversal of CFA-induced hyperalgesia.

4. Discussion

The driving force over the years in the opioid field has been the search for an alternative to morphine that would produce effective analgesia and would be free of undesirable side effects. New chemical approaches including the design of G protein-biased MOPr agonists and/or multifunctional ligands with mixed opioid and non-opioid activities for creating analgesics with fewer adverse effects are sought, and such drugs with improved benefit/risk profile are likely to have a significant impact [21; 24; 30].

In this study, we report the successful design and a thorough in vitro and in vivo characterization of two G protein-biased MOPr agonists, KGFF03 and KGFF09, possessing additional agonist and antagonist activities at NPFF1/2Rs, respectively. In vivo, they display potent antinociception with reduced respiratory depression after acute systemic (sc.) administration. The major finding of this study is that following chronic administration, KGFF09, but not KGFF03, produces effective antinociception with limited OIH and analgesic tolerance, as well as a reduced withdrawal syndrome, thus demonstrating the benefits of NPFFR system blockade towards MOPr agonists to limit the development of tolerance and dependence, the two major adverse effects associated with chronic administration of classical opiates.

Multitarget pharmacology, or polypharmacology, is defined as the specific binding of a compound to two or more molecular targets and relies on the observation that some biological networks are resilient to single-point perturbations, with redundant functions or compensatory mechanisms leading to the attenuation of the repeated perturbation (*i.e.* stimulation of the MOPr [22; 53]. Here, our strategy aimed at developing a dual acting drug combining the analgesic efficacy of opioid agonists, while blocking the NPFF1/2R. The pharmacological blockade of these two receptors with a mixed antagonist have previously been shown to improve adverse side effects associated with repeated exposure to opiates [14;

48]. As the respective role of NPFF1R and NPFF2R in the development of OIH and analgesic tolerance induced by chronic opiates is still unclear, we therefore favored compounds that target both NPFFR subtypes. To determine whether the NPFFR antagonist activity was responsible for the improved profile of KGFF09, we compared this MOPr-NPFFR hybrid peptidomimetic with its parent opioid agonist KGOP01, devoid of an NPFF pharmacophore (Fig. 1, Table S1). Both ligands show high affinity with a full agonist activity at MOPr, paralleled by effective and long-lasting acute analgesia. However, upon chronic administration to mice, KGOP01 rapidly induced analgesic tolerance and hyperalgesia, whereas KGFF09 did not. These results appear to oppose a recent report of a bifunctional MOP – NPFF agonist, BN9, that displayed acute and chronic analgesic efficacy [27]. However, this study also shows that when co-administered with BN9, the NPFF1/2R antagonist RF9 further potentiated the analgesic effect of BN9, thus questioning the benefit of the NPFF1/2R agonist activity on opioid analgesia. In addition, we describe KGFF03, a potent MOPr – NPFF1/2R agonist, which produces acute analgesia, while it also induces tolerance and hyperalgesia in an analogous manner to the parent opioid agonist KGOP01. Altogether, our data confirm the role of the NPFF system in the compensatory mechanisms triggered by the chronic opioid stimulation and further support the concept that blockade rather than activation of this system is beneficial to opioid analgesia following chronic administration.

We further demonstrated in a model of inflammatory pain the beneficial effect of NPFFRs inhibition on the development of analgesic tolerance and long-lasting inflammatory hyperalgesia. This delayed reversal of pain hypersensitivity induced by CFA observed with KGFF09 and not KGFF03 and KGOP1 suggests that the endogenous NPFF system could be activated upon administration of inflammatory agents, such as CFA, and that blocking this system can induce a progressive return to normal nociceptive sensitivity. This result is in

agreement with a recent report showing an upregulation of NPFF and NPFF2R mRNA in the spinal cord of mice treated with CFA or carrageenan [28]. Overall, our current data therefore indicate that activation of the NPFF system might represent a common feature in the development of hyperalgesia, whether induced by inflammation or repeated opioid stimulation.

Detailed in vitro characterization of the newly designed MOP-NPFF hybrids revealed that the addition of either -Arg-Phe-NH_2 (KGFF03) or -Bpa-Phe-NH_2 (KGFF09) to the *C*-terminus of the parent opioid structure KGOP01 not only conferred the expected NPFF1/2R affinity to the designed compounds, but also shows an advantageous switch of MOPr activity towards the G protein signaling over β-arrestin-2 recruitment. Studies on β-arrestin-2 knockout mice (β-arrestin-2 KO) report less opioid-associated adverse effects, such as respiratory depression, constipation, analgesic tolerance and physical dependence, as well as higher opioid antinociceptive effects [7]. Although KGFF03 and KGFF09 are not completely devoid of the β-arrestin-2 recruitment activity, their bias appeared sufficient for alleviating respiratory depression, compared to the unbiased MOPr agonist KGOP01. This result is in agreement with previous observations made with other G protein-biased MOPr agonists [10; 31]. KGOP01, KGFF03 and KGFF09 displayed similar gastrointestinal tract inhibitory effect, indicating that β-arrestin-2 is not involved in this adverse effect. Although we cannot exclude that this could be due to the residual β-arrestin-2 recruitment induced by KGFF03 and KGFF09, our observation is in agreement with recent reports questioning the effectiveness of G protein-biased MOPr agonists in such adverse effect [1; 25; 30]. The lower efficacy of KGFF09 to promote MOPr-induced β-arrestin-2 recruitment over G protein activation could also be reponsible for less analgesic tolerance and physical dependence. However, reports on the development of analgesic tolerance induced by opioids in β-arrestin-2 KO mice or following chronic treatments with G protein-biased MOPr agonists are conflicting [1; 6; 25].

Concerning physical dependence, the severity of antagonist-precipitated withdrawal response in β-arrestin-2 KO mice was reduced only when animals were chronically treated with low doses of morphine [43] and the biased MOPr agonist TRV130 was reported to induce similar withdrawal symptoms than morphine [50]. In this study, we show that KGFF03, having a biased activity on the MOPr, produces similar analgesic tolerance and physical dependence to the unbiased KGOP01 parent opioid agonist, suggesting that β-arrestin-2 bias is not critical for the development of these side effects.

Similarly to other biased MOPr agonists [10; 31], KGFF09 also binds to DOPr and KOPr, with DOPr agonist and KOPr antagonist activities. DOP agonists have been described to play no or limited analgesic activity in naive animals, but display potent anti-hyperalgesic activity in neuropathic and inflammatory pain models in rodents [17]. Although DOPr agonist activity is an interesting characteristic to consider when developing multitarget analgesic drugs, tolerance to DOPr-mediated analgesia has a very fast onset [42], which could limit the utility of this activity in chronic treatment. We also found that KGFF09 displays potent KOPr antagonist activity, a property also shared by PZM21, the recently described biased MOP agonist [31]. The KOPr has been shown to display anti-MOPr activity [3; 38], and its blockade could present synergism with MOPr and DOPr agonist activity, leading to the observed analgesic potency of KGFF09. Moreover, as DOPr agonists and KOPr antagonists have been shown to have an antidepressant potential [29], KGFF09 may have beneficial effects on the affective component of chronic pain syndromes.

In summary, we report here for the first time a dual acting, G protein biased MOPr agonist - NPFFRs antagonist, KGFF09. The association of both properties within a single molecule gathers the beneficial effects of biased MOPr agonists on acute side effects (respiratory depression) and those of NPFFRs antagonists on chronic side effects (OIH, tolerance and withdrawal syndrome), altogether leading to a potent analgesic with an

improved safety profile. Hence, our current findings pave the way to novel therapeutic strategies for the development of potent antinociceptive drugs with limited side effects upon both acute and chronic use.

Conflict of interest statement

A. Drieu la Rochelle, F. Bihel, M. Spetea, F. Simonin and S. Ballet have a related patent pending. The remaining authors have no conflict of interest to declare.

Acknowlegdments

We are grateful to the Integrative Biological Chemistry Platform (UMS 3286 CNRS, Illkirch, France) for technical assistance. This work was supported by the Centre National de la Recherche Scientifique, Université de Strasbourg, LABEX ANR-10-LABX-0034_Medalis funded by "Agence National de la Recherche" under "Programme d'investissement d'avenir", the Research Foundation Flanders (FWO Vlaanderen), the Strategic Research Program – Growth Funding of the VUB and the Austrian Science Fund (FWF: I 2463-B21).

References

[1] Altarifi AA, David B, Muchhala KH, Blough BE, Akbarali H, Negus SS. Effects of acute and repeated treatment with the biased mu opioid receptor agonist TRV130 (oliceridine) on measures of antinociception, gastrointestinal function, and abuse liability in rodents. J Psychopharmacol 2017;31(6):730-739.

[2] Ayachi S, Simonin F. Involvement of Mammalian RF-Amide Peptides and Their Receptors in the Modulation of Nociception in Rodents. Frontiers in endocrinology 2014;5:158.

[3] Bie B, Pan ZZ. Presynaptic mechanism for anti-analgesic and anti-hyperalgesic actions of kappa-opioid receptors. J Neurosci 2003;23(19):7262-7268.

[4] Bihel F. Opioid adjuvant strategy: improving opioid effectiveness. Future medicinal chemistry 2016;8(3):339-354.

[5] Bihel F, Humbert JP, Schneider S, Bertin I, Wagner P, Schmitt M, Laboureyras E, Petit-Demouliere B, Schneider E, Mollereau C, Simonnet G, Simonin F, Bourguignon JJ. Development of a peptidomimetic antagonist of neuropeptide FF receptors for the prevention of opioid-induced hyperalgesia. ACS chemical neuroscience 2015;6(3):438-445.

[6] Bohn LM, Gainetdinov RR, Lin FT, Lefkowitz RJ, Caron MG. Mu-opioid receptor desensitization by beta-arrestin-2 determines morphine tolerance but not dependence. Nature 2000;408(6813):720-723.

[7] Bohn LM, Lefkowitz RJ, Gainetdinov RR, Peppel K, Caron MG, Lin FT. Enhanced morphine analgesia in mice lacking beta-arrestin 2. Science (New York, NY 1999;286(5449):2495-2498.

[8] Celerier E, Rivat C, Jun Y, Laulin JP, Larcher A, Reynier P, Simonnet G. Long-lasting hyperalgesia induced by fentanyl in rats: preventive effect of ketamine. Anesthesiology 2000;92(2):465-472.

[9] Chou R, Turner JA, Devine EB, Hansen RN, Sullivan SD, Blazina I, Dana T, Bougatsos C, Deyo RA. The effectiveness and risks of long-term opioid therapy for chronic pain: a systematic review for a National Institutes of Health Pathways to Prevention Workshop. Annals of internal medicine 2015;162(4):276-286.

[10] DeWire SM, Yamashita DS, Rominger DH, Liu G, Cowan CL, Graczyk TM, Chen XT, Pitis PM, Gotchev D, Yuan C, Koblish M, Lark MW, Violin JD. A G protein-biased ligand at the mu-opioid receptor is potently analgesic with reduced gastrointestinal and respiratory dysfunction compared with morphine. The Journal of pharmacology and experimental therapeutics 2013;344(3):708-717.

[11] Ding H, Czoty PW, Kiguchi N, Cami-Kobeci G, Sukhtankar DD, Nader MA, Husbands SM, Ko MC. A novel orvinol analog, BU08028, as a safe opioid analgesic without abuse liability in primates. Proceedings of the National Academy of Sciences of the United States of America 2016;113(37):E5511-5518.

[12] Elhabazi K, Ayachi S, Ilien B, Simonin F. Assessment of morphine-induced hyperalgesia and analgesic tolerance in mice using thermal and mechanical nociceptive modalities. Journal of visualized experiments : JoVE 2014(89):e51264.

[13] Elhabazi K, Humbert JP, Bertin I, Schmitt M, Bihel F, Bourguignon JJ, Bucher B, Becker JA, Sorg T, Meziane H, Petit-Demouliere B, Ilien B, Simonin F. Endogenous mammalian RF-amide peptides, including PrRP, kisspeptin and 26RFa, modulate nociception and morphine analgesia via NPFF receptors. Neuropharmacology 2013;75C:164-171.

[14] Elhabazi K, Trigo JM, Mollereau C, Mouledous L, Zajac JM, Bihel F, Schmitt M, Bourguignon JJ, Meziane H, Petit-demouliere B, Bockel F, Maldonado R, Simonin F. Involvement of neuropeptide FF receptors in neuroadaptive responses to acute and chronic opiate treatments. British journal of pharmacology 2012;165(2):424-435.

[15] Eriksen J, Sjogren P, Bruera E, Ekholm O, Rasmussen NK. Critical issues on opioids in chronic non-cancer pain: an epidemiological study. Pain 2006;125(1-2):172-179.

[16] Findeisen M, Rathmann D, Beck-Sickinger AG. Structure-activity studies of RFamide peptides reveal subtype-selective activation of neuropeptide FF1 and FF2 receptors. ChemMedChem 2011;6(6):1081-1093.

[17] Gaveriaux-Ruff C, Kieffer BL. Delta opioid receptor analgesia: recent contributions from pharmacology and molecular approaches. Behavioural pharmacology 2011;22(5-6):405-414.

[18] Gealageas R, Schneider S, Humbert J-P, Bertin I, Schmitt M, Laboureyras E, Dugave C, Mollereau C, Simonnet G, Bourguignon J-J, Simonin F, Bihel F. Development of sub-nanomolar dipeptidic ligands of neuropeptide FF receptors. Bioorganic & medicinal chemistry letters 2012;22(24):7471-7474.

[19] Grosser T, Woolf CJ, FitzGerald GA. Time for nonaddictive relief of pain. Science (New York, NY) 2017;355(6329):1026-1027.

[20] Guillemyn K, Kleczkowska P, Lesniak A, Dyniewicz J, Van der Poorten O, Van den Eynde I, Keresztes A, Varga E, Lai J, Porreca F, Chung NN, Lemieux C, Mika J, Rojewska E, Makuch W, Van Duppen J, Przewlocka B, Vanden Broeck J, Lipkowski AW, Schiller PW, Tourwe D, Ballet S. Synthesis and biological evaluation of compact, conformationally constrained bifunctional opioid agonist - neurokinin-1 antagonist peptidomimetics. European journal of medicinal chemistry 2015;92:64-77.

[21] Gunther T, Dasgupta P, Mann A, Miess E, Kliewer A, Fritzwanker S, Steinborn R, Schulz S. Targeting multiple opioid receptors - improved analgesics with reduced side effects? British journal of pharmacology, in press.

[22] Hopkins AL. Network pharmacology: the next paradigm in drug discovery. Nature chemical biology 2008;4(11):682-690.

[23] Journigan VB, Mesangeau C, Vyas N, Eans SO, Cutler SJ, McLaughlin JP, Mollereau C, McCurdy CR. Nonpeptide small molecule agonist and antagonist original leads for neuropeptide FF1 and FF2 receptors. Journal of medicinal chemistry 2014;57(21):8903-8927.

[24] Kleczkowska P, Lipkowski AW, Tourwe D, Ballet S. Hybrid opioid/non-opioid ligands in pain research. Current pharmaceutical design 2013;19(42):7435-7450.

[25] Koblish M, Carr R, 3rd, Siuda ER, Rominger DH, Gowen-MacDonald W, Cowan CL, Crombie AL, Violin JD, Lark MW. TRV0109101, a G Protein-Biased Agonist of the micro-Opioid Receptor, Does Not Promote Opioid-Induced Mechanical Allodynia following Chronic Administration. The Journal of pharmacology and experimental therapeutics 2017;362(2):254-262.

[26] Lattanzi R, Spetea M, Schullner F, Rief SB, Krassnig R, Negri L, Schmidhammer H. Synthesis and biological evaluation of 14-alkoxymorphinans. 22.(1) Influence of the 14-alkoxy group and the substitution in position 5 in 14-alkoxymorphinan-6-ones on in vitro and in vivo activities. Journal of medicinal chemistry 2005;48(9):3372-3378.

[27] Li N, Han ZL, Wang ZL, Xing YH, Sun YL, Li XH, Song JJ, Zhang T, Zhang R, Zhang MN, Xu B, Fang Q, Wang R. BN-9, a chimeric peptide with mixed opioid and neuropeptide FF receptor agonistic properties, produces nontolerance-forming antinociception in mice. British journal of pharmacology 2016;173(11):1864-1880.

[28] Lin YT, Liu HL, Day YJ, Chang CC, Hsu PH, Chen JC. Activation of NPFFR2 leads to hyperalgesia through the spinal inflammatory mediator CGRP in mice. Experimental neurology 2017;291:62-73.

[29] Lutz PE, Kieffer BL. Opioid receptors: distinct roles in mood disorders. Trends in neurosciences 2013;36(3):195-206.

[30] Madariaga-Mazon A, Marmolejo-Valencia AF, Li Y, Toll L, Houghten RA, Martinez-Mayorga K. Mu-Opioid receptor biased ligands: A safer and painless discovery of analgesics? Drug discovery today 2017;22(11):1719-1729.

[31] Manglik A, Lin H, Aryal DK, McCorvy JD, Dengler D, Corder G, Levit A, Kling RC, Bernat V, Hubner H, Huang XP, Sassano MF, Giguere PM, Lober S, Da D, Scherrer G, Kobilka BK, Gmeiner P, Roth BL, Shoichet BK. Structure-based discovery of opioid analgesics with reduced side effects. Nature 2016;537(7619):185-190.

[32] Matsumoto K, Narita M, Muramatsu N, Nakayama T, Misawa K, Kitajima M, Tashima K, Devi LA, Suzuki T, Takayama H, Horie S. Orally active opioid mu/delta dual agonist MGM-16, a derivative of the indole alkaloid mitragynine, exhibits potent antiallodynic effect on neuropathic pain in mice. The Journal of pharmacology and experimental therapeutics 2014;348(3):383-392.

[33] Mazarguil H, Gouarderes C, Tafani JA, Marcus D, Kotani M, Mollereau C, Roumy M, Zajac JM. Structure-activity relationships of neuropeptide FF: role of C-terminal regions. Peptides 2001;22(9):1471-1478.

[34] Michel G, Matthes HW, Hachet-Haas M, El Baghdadi K, de Mey J, Pepperkok R, Simpson JC, Galzi JL, Lecat S. Plasma membrane translocation of REDD1 governed by GPCRs contributes to mTORC1 activation. Journal of cell science 2014;127(Pt 4):773-787.

[35] Nguyen T, Decker AM, Langston TL, Mathews KM, Siemian JN, Li JX, Harris DL, Runyon SP, Zhang Y. Discovery of Novel Proline-Based Neuropeptide FF Receptor Antagonists. ACS chemical neuroscience 2017;8(10):2290-2308.

[36] Novoa A, Van Dorpe S, Wynendaele E, Spetea M, Bracke N, Stalmans S, Betti C, Chung NN, Lemieux C, Zuegg J, Cooper MA, Tourwe D, De Spiegeleer B, Schiller PW, Ballet S. Variation of the net charge, lipophilicity, and side chain flexibility in Dmt(1)-DALDA: Effect on Opioid Activity and Biodistribution. Journal of medicinal chemistry 2012;55(22):9549-9561.

[37] Olson KM, Lei W, Keresztes A, LaVigne J, Streicher JM. Novel Molecular Strategies and Targets for Opioid Drug Discovery for the Treatment of Chronic Pain. The Yale journal of biology and medicine 2017;90(1):97-110.

[38] Pan ZZ. mu-Opposing actions of the kappa-opioid receptor. Trends in pharmacological sciences 1998;19:94-98.

[39] Papaleo F, Contarino A. Gender- and morphine dose-linked expression of spontaneous somatic opiate withdrawal in mice. Behavioural brain research 2006;170(1):110-118.

[40] Pasternak GW, Pan YX. Mu opioids and their receptors: evolution of a concept. Pharmacological reviews 2013;65(4):1257-1317.

[41] Pradhan AA, Becker JA, Scherrer G, Tryoen-Toth P, Filliol D, Matifas A, Massotte D, Gaveriaux-Ruff C, Kieffer BL. In vivo delta opioid receptor internalization controls behavioral effects of agonists. PloS one 2009;4(5):e5425.

[42] Pradhan AA, Walwyn W, Nozaki C, Filliol D, Erbs E, Matifas A, Evans C, Kieffer BL. Ligand-directed trafficking of the delta-opioid receptor in vivo: two paths toward analgesic tolerance. J Neurosci 2010;30(49):16459-16468.

[43] Raehal KM, Bohn LM. beta-arrestins: regulatory role and therapeutic potential in opioid and cannabinoid receptor-mediated analgesia. Handbook of experimental pharmacology 2014;219:427-443.

[44] Raehal KM, Walker JK, Bohn LM. Morphine side effects in beta-arrestin 2 knockout mice. The Journal of pharmacology and experimental therapeutics 2005;314(3):1195-1201.

[45] Roeckel LA, Utard V, Reiss D, Mouheiche J, Maurin H, Robe A, Audouard E, Wood JN, Goumon Y, Simonin F, Gaveriaux-Ruff C. Morphine-induced hyperalgesia involves mu opioid receptors and the metabolite morphine-3-glucuronide. Scientific reports 2017;7(1):10406.

[46] Schneider S, Ftouni H, Niu S, Schmitt M, Simonin F, Bihel F. Rapid and scalable synthesis of innovative unnatural alpha,beta or gamma-amino acids functionalized with tertiary amines on their side-chains. Organic & biomolecular chemistry 2015;13(25):7020-7026.

[47] Simonin F. Neuropeptide FF receptors as therapeutic targets. Drugs Future 2006;31(7):603-609.

[48] Simonin F, Schmitt M, Laulin J-P, Laboureyras E, Jhamandas JH, MacTavish D, Matifas A, Mollereau C, Laurent P, Parmentier M, Kieffer BL, Bourguignon J-J, Simonnet G. RF9, a potent and selective neuropeptide FF receptor antagonist, prevents opioid-induced tolerance associated with hyperalgesia. Proc Natl Acad Sci USA 2006;103(2):466-471.

[49] Simonin F, Valverde O, Smadja S, Slowe S, Kitchen I, Dierich A, Le Meur M, Roques BP, Maldonado R, Kieffer BL. Disruption of the k-opioid receptor gene in mice enhances sensitivity to chemical visceral pain, impairs pharmacological actions of the selective k-agonist U-50,488H and attenuates morphine withdrawal. EMBO J 1998;17:886-897.

[50] Siuda ER, Carr R, 3rd, Rominger DH, Violin JD. Biased mu-opioid receptor ligands: a promising new generation of pain therapeutics. Curr Opin Pharmacol 2017;32:77-84.

[51] Spetea M, Bohotin CR, Asim MF, Stubegger K, Schmidhammer H. In vitro and in vivo pharmacological profile of the 5-benzyl analogue of 14-methoxymetopon, a novel mu opioid analgesic with reduced propensity to alter motor function. European journal of pharmaceutical sciences : official journal of the European Federation for Pharmaceutical Sciences 2010;41(1):125-135.

[52] Starnowska J, Guillemyn K, Makuch W, Mika J, Ballet S, Przewlocka B. Bifunctional opioid/nociceptin hybrid KGNOP1 effectively attenuates pain-related behaviour in a rat model of neuropathy. European journal of pharmaceutical sciences : official journal of the European Federation for Pharmaceutical Sciences 2017;104:221-229.

[53] Talevi A. Multi-target pharmacology: possibilities and limitations of the "skeleton key approach" from a medicinal chemist perspective. Frontiers in pharmacology 2015;6:205.

[54] Tan PP, Chen JC, Li JY, Liang KW, Wong CH, Huang EY. Modulation of naloxone-precipitated morphine withdrawal syndromes in rats by neuropeptide FF analogs. Peptides 1999;20(10):1211-1217.

[55] Von Korff M, Saunders K, Thomas Ray G, Boudreau D, Campbell C, Merrill J, Sullivan MD, Rutter CM, Silverberg MJ, Banta-Green C, Weisner C. De facto long-term opioid therapy for noncancer pain. The Clinical journal of pain 2008;24(6):521-527.

[56] Yang HY, Fratta W, Majane EA, Costa E. Isolation, sequencing, synthesis, and pharmacological characterization of two brain neuropeptides that modulate the action of morphine. Proceedings of the National Academy of Sciences of the United States of America 1985;82(22):7757-7761.

Figure legends

Figure 1: Design strategy and in vitro screening of KGFF peptidomimetics for affinity at MOPr, NPFF1R and NPFF2R.

A: KGFF compounds combining the opioid ligand KGOP01 and NPFF ligand pharmacophores. From this strategy, 16 compounds were synthetized and screened in vitro for their affinity for the MOPr, NPFF1R and NPFF2R.

B: Chemical diversity at the NPFF ligand pharmacophore with Arg mimetics / Orn derivatives serving as Arg mimetics for the NPFF ligand pharmacophore.

C: Binding affinity constants (pK_i values) were determined in radioligand competition binding assays with membranes from CHO cells expressing hMOPr, hNPFF1R or hNPFF2R. Values are mean ± SEM of at least 2 independent experiments performed in duplicate. See also Table S1.

Figure 2: In vitro functional characterization of KGFF peptidomimetics.

A: Inhibition of forskolin-induced cAMP accumulation in HEK293-Glo20F-hMOPr cells.

B, E: hNPFF1R activation measured by [^{35}S]-GTPγS binding with membranes from CHO-hNPFF1R cells.

C, F: hNPFF2R activation measured by [^{35}S]-GTPγS binding with membranes from CHO-hNPFF2R cells.

D: eYFP-labelled β-arrestin-2 translocation to Rluc-hMOPr in HEK293 cells. Agonist specific BRET1 ratio were determined by subtracting BRET1 ratio of non-activated cells, and normalized to the maximal effect of DAMGO.

(A, B, C) Potency constants (pEC_{50}) and efficacy values (E_{max}) are shown on left panels and representative experiments for KGOP01, KGFF03 and KGFF09 on right panels, see also Table S2. Efficacy values (E_{max}) are relative to DAMGO **(A)**, RFRP3 **(B)** or NPFF **(C)** response. NPFF1R **(E)** and NPFF2R **(F)** antagonisms were assessed with RFRP3 or NPFF

dose-response curve, respectively, in the presence of increasing KGFF09 concentrations, see also Figure S1. Values are mean ± SEM of at least 2 independent experiments performed in duplicate or triplicate.

Figure 3: Antinociceptive effect of KGOP01, KGFF03 and KGFF09 after acute sc. administration to mice.

A: Time- and dose-dependent analgesic effects of KGOP01, KGFF03 and KGFF09 in the tail immersion test after sc. administration in C57BL/6N mice. Withdrawal latencies are expressed in seconds and presented as mean ± SEM (n = 6-7).

B: Time- and dose-dependent analgesic effects of KGOP01, KGFF03 and KGFF09 in the radiant tail-flick test after sc. administration in CD1 mice. Tail-flick latencies (as %MPE) are shown as mean ± SEM (n = 6-8).

Figure 4: Adaptive responses induced by KGOP01, KGFF03 and KGFF09 after chronic sc. treatment of mice.

A: Development of hyperalgesia and analgesic tolerance upon chronic treatment with KGOP01, KGFF03 and KGFF09. C57BL/6N mice received daily (d1 to d8) injections of KGOP01 (1.8 µmol/kg, sc.), KGFF03 (1.2 µmol/kg, sc.), KGFF09 (7.4 µmol/kg, sc.) or saline (**A, B, C)**.

B: Development of hyperalgesia upon chronic treatment of C57BL/6N mice with KGOP01, KGFF03 and KGFF09. Basal nociceptive values were measured for two days before drug treatment and once daily before drug administration (d1 to d8), using the tail immersion test. Each day of injection is shown with an arrowhead.

C: Development of analgesic tolerance upon chronic treatment of C57BL/6N mice with KGOP01, KGFF03 and KGFF09. Comparison between groups of area-under-the-curve

(AUC) values over the 0-7h time course is shown on the left panel and development of tolerance (%) at day 8 relative to day 1 on the right panel.

D: Effect of KGOP01, KGFF03 or KGFF09 on naltrexone-precipitated withdrawal signs after chronic treatment of C57BL/6N mice. The different signs of withdrawal were measured over 30 min immediately after naltrexone injection (1 mg/kg, sc.) and a global withdrawal score (GWS) was calculated. KGOP01 (1.8 µmol/kg, sc.), KGFF03 (1.2 µmol/kg, sc.) and KGFF09 (7.4 µmol/kg, sc.) were administered twice daily for 7 days. See also Figure S3.

E: Effect of KGOP01, KGFF03 and KGFF09 on respiratory frequency after sc. administration to C57BL/6N mice, measured by whole body mouse plethysmography immediately after injection of KGOP01 (1.8 µmol/kg, sc.), KGFF03 (1.2 µmol/kg, sc.), KGFF09 (7.4 µmol/kg, sc.) or saline (sc.). Comparison between groups of respiratory frequency (left panel) and area-under-the curve (AUC, right panel) values over the 100 min kinetics are shown.

Data are expressed as mean ± SEM. Groups were compared using one-way (**C** right panel, and **D**, **E** right panel) or two-way (**B**, **C** left panel, and **E** left panel) ANOVA with Bonferroni post hoc test *p<0.05, **p<0.01, ***p<0.001 as compared to saline, ##p<0.01 as compared to KGOP01, +p<0.001 as compared to KGFF09.

Figure 5: KGFF09 induces antinociception with reduced tolerance and anti-hyperalgesia in mice with inflammatory pain.

C57BL/6N mice were injected on day 1 with CFA or saline in the tail, and then daily administered with KGOP01 (1.8 µmol/kg/d, sc.), KGFF03 (1.2 µmol/kg/d, sc.), KGFF09 (7.4 µmol/kg/d, sc.) or saline (sc., CFA/saline and saline/saline).

A: Analgesic tolerance to the thermal antinociceptive effect was measured 2 h after daily sc. administration on days 2 – 3 – 5 – 7 by the tail immersion test. Comparison between groups of the %MPE (left panel) and tolerance (%) at day 7 relative to day 2 (right panel) are shown.

B: Analgesic tolerance to the mechanical antinociceptive effect was measured 2 h after daily sc. injection on days 2 – 4 – 6 – 8 by the tail pressure test. Comparison between groups of percentage of the %MPE (left panel) and tolerance (%) at day 8 relative to day 2 (right panel) are shown.

C, D: Anti-hyperalgesic activity of KGOP01, KGFF03 and KGFF09. Basal nociceptive thresholds were measured by the tail immersion test (C) or tail pressure test (D) once daily before drug administration to visualize CFA-induced pain hypersensitivity.

Data are expressed as mean ± SEM, n = 8-10. Statistical significance was calculated with two-way ANOVA with Bonferroni post hoc test *p<0.5, **p<0.01, ***p<0.001 vs saline mice, +p<0.5, ++p<0.01, +++p<0.001 vs KGOP01, and with one-way ANOVA with Bonferroni post hoc test ###p<0.001 vs KGFF09.

Tables

Table 1: Structure of the different compounds designed and characterized in this study

Compound	**Sequence**					
position	1	2	3	4	5	6
KGFF01	H-Dmt	D-Arg	Aba	Gly	Arg	Phe-NH_2
KGFF02	H-Dmt	D-Arg	Aba	Gly	Arg	Phe-OH
KGFF03	H-Dmt	D-Arg	Aba	β-Ala	Arg	Phe-NH_2
KGFF04	H-Dmt	D-Arg	Aba	Gly	Orn	Phe-NH_2
KGFF05	H-Dmt	D-Arg	-	Phe	Orn	Phe-NH_2
KGFF06	H-Dmt	L-Arg	-	-	-	Phe-NH_2
KGFF07	H-Dmt	D-Arg	-	-	-	Phe-NH_2

KGFF08	H-Dmt	D-Arg	Aba	β-Ala	Apa	Phe-NH_2
KGFF09	H-Dmt	D-Arg	Aba	β-Ala	Bpa	Phe-NH_2
KGFF10	H-Dmt	-	-	-	Apa	Phe-NH_2
KGFF11	H-Dmt	-	-	-	Bpa	Phe-NH_2
KGFF12	H-Dmt	D-Arg	Aba-NH	-	-	-
KGFF13	H-Dmt	D-Arg	-	-	-	Phe-NH-CH_3
KGFF14	H-Dmt	D-Arg	Aba	β-Ala	Lys(Bim)	Phe-NH_2
KGFF15	H-Dmt	D-Arg	Aba	β-Ala	Lys(Box)	Phe-NH_2
KGFF16	H-Dmt	D-Arg	Aba	β-Ala	Lys(Bth)	Phe-NH_2
KGOP01	H-Dmt	D-Arg	Aba	β-Ala- NH_2		

Table 2: Binding affinity constant (K_i) values and activity agonist constant (EC_{50} and E_{max}) values of KGFF compounds for human DOPr, KOPr and NOPr.

compound	**DOPr** (cAMP)			**KOPr** (cAMP)			**NOPr** (cAMP)		
	K_i (nM)	**EC_{50} (nM)**	**E_{max} (%)**	**K_i (nM)**	**EC_{50} (nM)**	**E_{max} (%)**	**K_i (nM)**	**EC_{50} (nM)**	**E_{max} (%)**
Naloxone	15.9 ± 2.3			8.4 ± 4.3					
DPDPE	57.1 ± 18.8	0.8 ± 0.3	100 ± 11	nd	nd	nd	nd	nd	nd
Dynorphin A	nd	nd	nd	nd	1.0 ± 0.4	100 ± 14	nd	nd	nd
Nociceptin	nd	nd	nd	nd	nd	nd	0.0013 ± 0.0002	0.568 ± 0.004	100 ± 3
KGOP01	5.1 ± 0.5	0.16 ± 0.01	91 ± 2	37.3 ± 9.6	> 10,000	18 ± 1	> 10,000	nd	nd
KGFF03	9.1 ± 0.7	0.34 ± 0.12	89 ± 6	108 ± 28	95 ± 3	34 ± 11	289 ± 3	> 10,000	15 ± 2
KGFF09	186 ± 77	0.78 ± 0.01	90 ± 3	3.2 ± 0.8	> 10,000	15 ± 1	209 ± 2	> 10,000	7 ± 3

K_i values were determined from competition binding curves using [^{3}H]-diprenorphine for DOPr and KOPr and [^{3}H]-nociceptin for NOPr. Efficacy (E_{max}) is expressed as the percentage relative to the reference agonists (DPDPE, dynorphin A and nociceptin for DOPr, KOPr and NOPr, respectively). Data are mean ± SEM of at least two independent experiments performed in duplicate. nd, not determined.

Table 3: Antinociceptive potencies of KGOP01, KGFF03 and KGFF09 in comparison to morphine in the radiant heat tail-flick test

compound	**ED_{50}, µmol/kg (95% confidence limits)[a]**	**relative potency to morphine**
morphine[b]	6.6 (3.5 – 12.6)	1
KGOP01	0.53 (0.25 – 1.1)	12
KGFF03	0.77 (0.52 – 1.2)	8.6
KGFF09	2.4 (1.3 – 4.5)	2.8

[a]ED_{50} were determined in CD1 mice (n = 6-8) after sc. drug administration at the peak effect (i.e. 1 h for KGOP01 and KGFF09, and 2 h for KGFF03).

[b]Data from (Novoa et al., 2012).

Figures

Figure 1

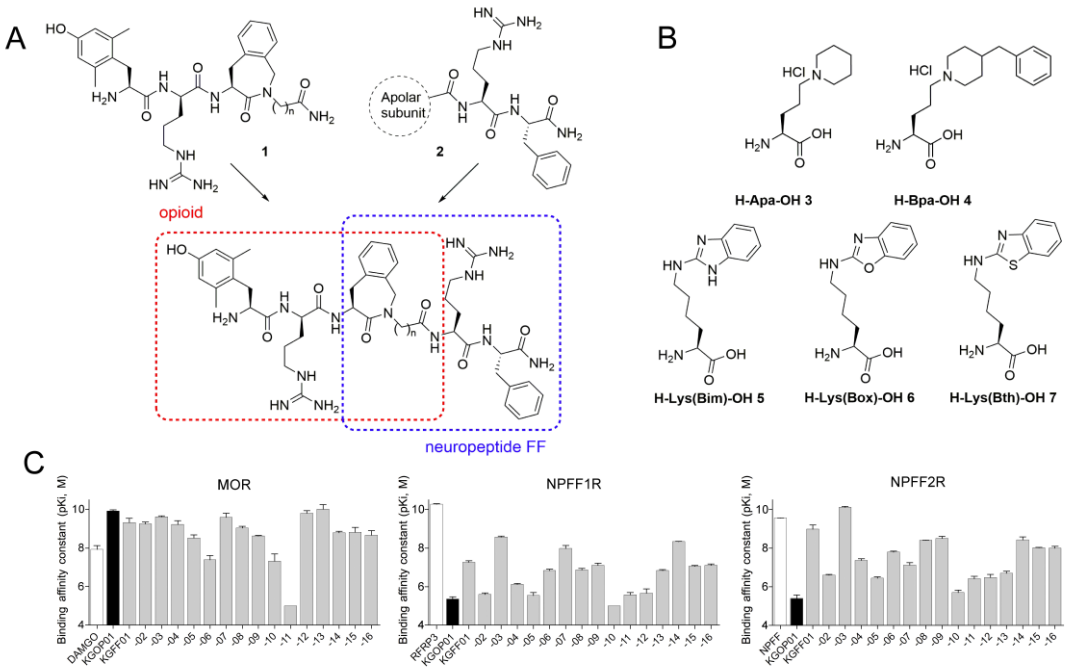

Figure 2

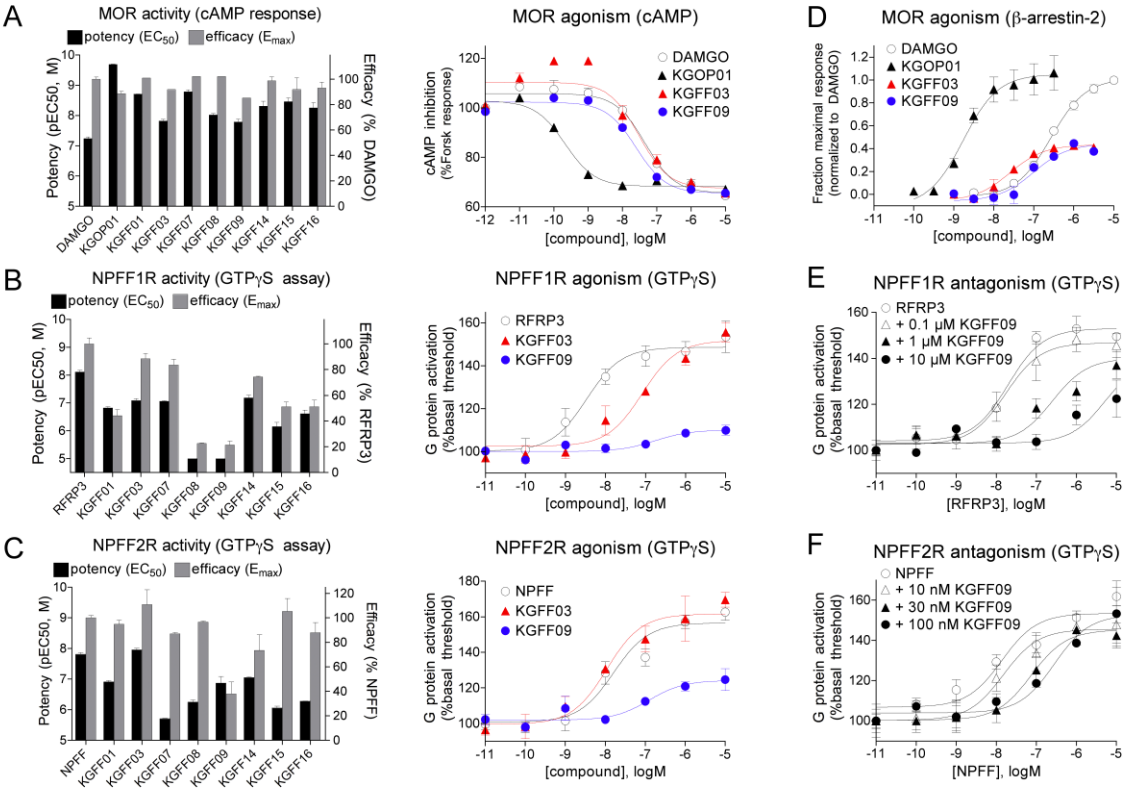
A
MOR activity (cAMP response)
potency (EC50)
efficacy (Emax)
Potency (pEC50, M)
Efficacy (% DAMGO)
DAMGO
KGOP01
KGFF01
KGFF03
KGFF07
KGFF08
KGFF09
KGFF14
KGFF15
KGFF16
MOR agonism (cAMP)
cAMP inhibition (%Forsk response)
[compound], logM
D
MOR agonism (β-arrestin-2)
Fraction maximal response (normalized to DAMGO)
B
NPFF1R activity (GTPγS assay)
Efficacy (% RFRP3)
RFRP3
NPFF1R agonism (GTPγS)
G protein activation (%basal threshold)
E
NPFF1R antagonism (GTPγS)
+ 0.1 μM KGFF09
+ 1 μM KGFF09
+ 10 μM KGFF09
[RFRP3], logM
C
NPFF2R activity (GTPγS assay)
Efficacy (% NPFF)
NPFF
NPFF2R agonism (GTPγS)
F
NPFF2R antagonism (GTPγS)
+ 10 nM KGFF09
+ 30 nM KGFF09
+ 100 nM KGFF09
[NPFF], logM

Figure 3

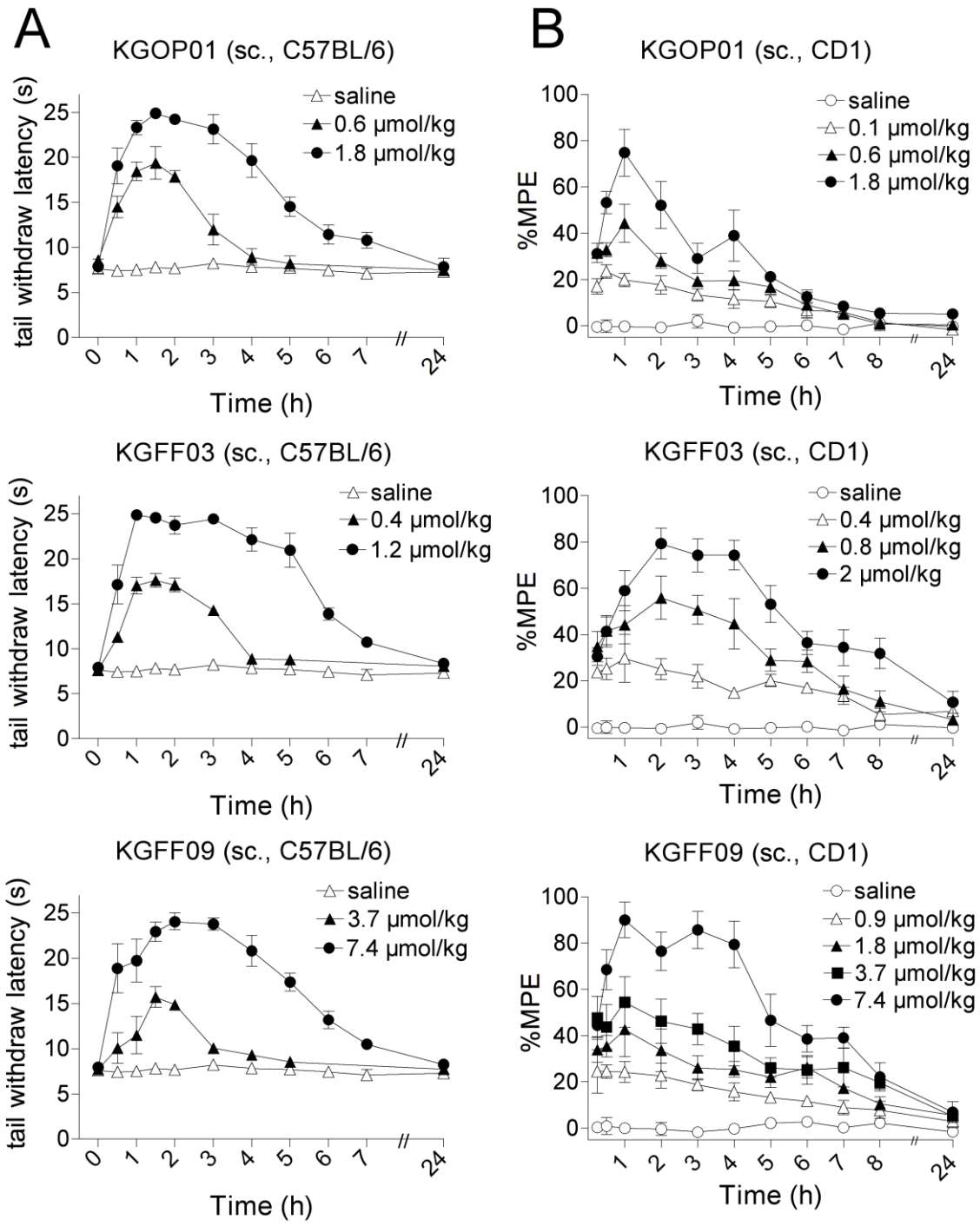
A
KGOP01 (sc., C57BL/6)
tail withdraw latency (s)
saline
0.6 µmol/kg
1.8 µmol/kg
Time (h)
B
KGOP01 (sc., CD1)
%MPE
saline
0.1 µmol/kg
0.6 µmol/kg
1.8 µmol/kg
Time (h)
KGFF03 (sc., C57BL/6)
tail withdraw latency (s)
saline
0.4 µmol/kg
1.2 µmol/kg
Time (h)
KGFF03 (sc., CD1)
%MPE
saline
0.4 µmol/kg
0.8 µmol/kg
2 µmol/kg
Time (h)
KGFF09 (sc., C57BL/6)
tail withdraw latency (s)
saline
3.7 µmol/kg
7.4 µmol/kg
Time (h)
KGFF09 (sc., CD1)
%MPE
saline
0.9 µmol/kg
1.8 µmol/kg
3.7 µmol/kg
7.4 µmol/kg
Time (h)

Figure 4

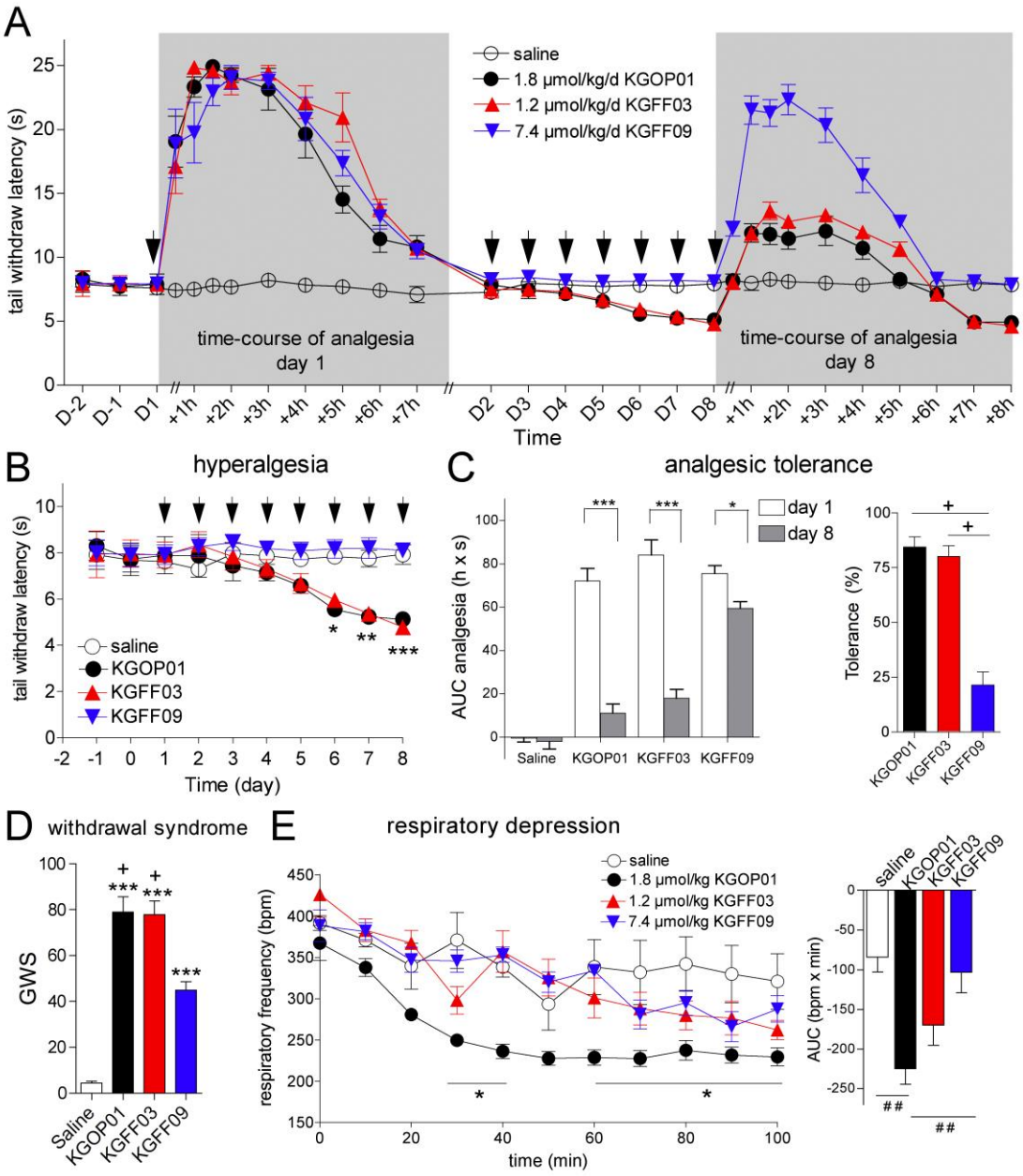
A
tail withdraw latency (s)
saline
1.8 µmol/kg/d KGOP01
1.2 µmol/kg/d KGFF03
7.4 µmol/kg/d KGFF09
time-course of analgesia day 1
time-course of analgesia day 8
Time
B
hyperalgesia
tail withdraw latency (s)
saline
KGOP01
KGFF03
KGFF09
Time (day)
C
analgesic tolerance
AUC analgesia (h x s)
day 1
day 8
Saline
KGOP01
KGFF03
KGFF09
Tolerance (%)
D
withdrawal syndrome
GWS
E
respiratory depression
respiratory frequency (bpm)
saline
1.8 µmol/kg KGOP01
1.2 µmol/kg KGFF03
7.4 µmol/kg KGFF09
time (min)
AUC (bpm x min)

Figure 5

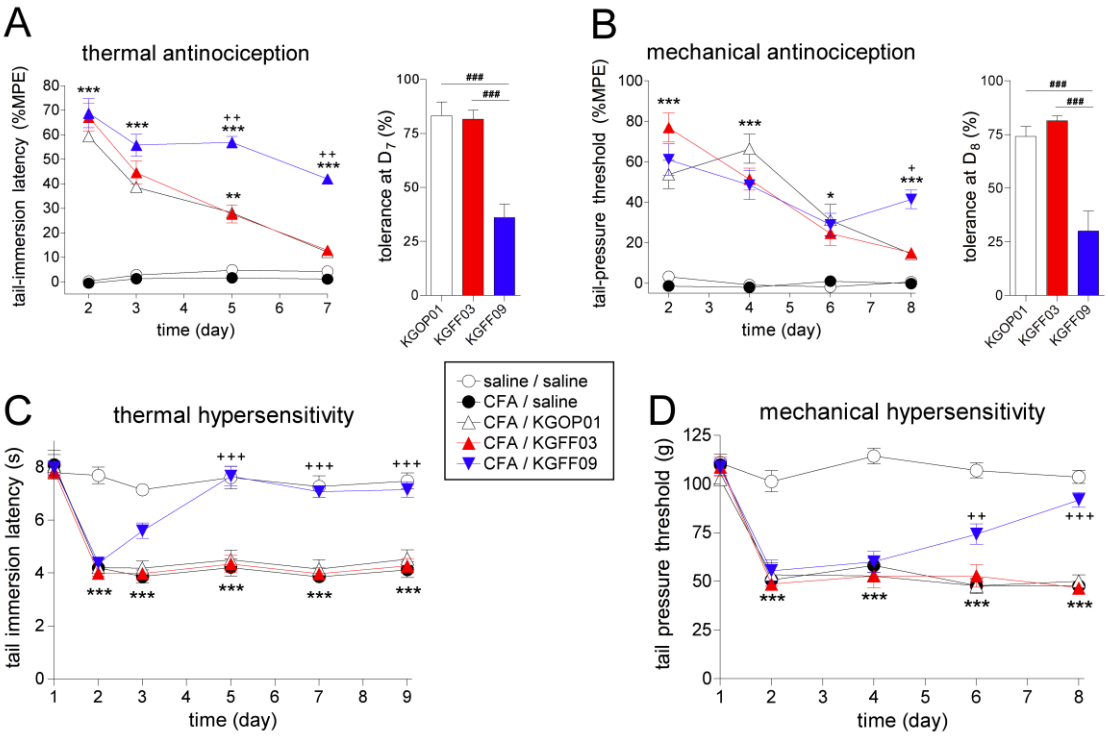
A
thermal antinociception
tail-immersion latency (%MPE)
time (day)
tolerance at D7 (%)
KGOP01
KGFF03
KGFF09
B
mechanical antinociception
tail-pressure threshold (%MPE)
time (day)
tolerance at D8 (%)
saline / saline
CFA / saline
CFA / KGOP01
CFA / KGFF03
CFA / KGFF09
C
thermal hypersensitivity
tail immersion latency (s)
time (day)
D
mechanical hypersensitivity
tail pressure threshold (g)
time (day)

Supplemental Digital Content:

Materials and Methods Supplemental Digital Content 1, which describes peptide characterization and synthesis of the arginine mimetics and ornithine mimetics.

Table Supplemental Digital Content 2, which summarize affinity constant (K_i) values of KGFF compounds for MOPr, NPFF1R, and NPFF2R.

Table Supplemental Digital Content 3, which summarize agonist activity constants (EC_{50} and E_{max}) values of KGFF compounds for MOPr, NPFF1R, and NPFF2R.

Figure Supplemental Digital Content 4, which shows in vitro characterization of KGFF03 and KGFF09 on NPFFRs.

Figure Supplemental Digital Content 5, which shows the robustness of β-arrestin-2 recruitment to MOR induced by DAMGO.

Figure Supplemental Digital Content 6, which shows in vitro characterization of KGOP01, KGFF03 and KGFF09 on opioid receptors.

Table Supplemental Digital Content 7, which summarize affinity constant (K_i) values of KGFF compounds for GPR10, GPR54 and GPR103.

Figure Supplemental Digital Content 8, which shows effect of KGOP01, KGFF03 and KGFF09 on naltrexone-precipitated withdrawal signs after chronic exposure in mice.

Figure Supplemental Digital Content 9, which shows effect of KGOP01, KGFF03 and KGFF09 on gastro-intestinal motility and motor coordination.

Figure Supplemental Digital Content 10, which shows acute antinociceptive time course of KGOP01, KGFF03 and KGFF09 in CFA-induced pain mode